Characterization of the Aggregates Made by Short Poly(ethylene oxide) Chains Labeled at One End with Pyrene

Howard Siu, Telmo J. V. Prazeres, and Jean Duhamel*

Institute of Polymer Research, Department of Chemistry, University of Waterloo, Waterloo ON N2L 3G1, Canada

Keith Olesen and Greg Shay

The Dow Chemical Company, UCAR Emulsion Systems, 410 Gregson Drive, Cary, North Carolina 27511

Received October 4, 2004; Revised Manuscript Received January 14, 2005

ABSTRACT: The association of a monodisperse poly(ethylene oxide) 53 ethylene oxide units long and labeled at one end with pyrene (Py-PEO) was monitored as a function of Py-PEO concentration by steady-state and time-resolved fluorescence, surface tension, static (SLS), and dynamic (DLS) light scattering. The excimer fluorescence decays exhibit no rise time for any polymer concentration investigated in this study (>0.5 g/L), indicating that pyrene aggregates are present in solution and confirming the existence of Py-PEO micelles. No excimer emission could be detected for Py-PEO concentration smaller than 0.1 g/L. The first critical aggregation concentration (CAC1) for the formation of Py-PEO micelles was estimated to equal 0.003 g/L by SLS. The Py-PEO micelles are surface active above a Py-PEO concentration larger than 0.001 g/L (0.4 μM) where a clear drop in surface tension is observed at concentrations slightly lower than CAC1. At a Py-PEO concentration of 10 g/L, the surface tension plateaus due to the aggregation of Py-PEO micelles. This corresponds to a second critical aggregation concentration referred to as CAC2. The aggregation was probed by DLS. DLS provided the hydrodynamic diameter of the Py-PEO micelles, which was found to equal 7.2 ± 3.1 nm. Fluorescence was used to determine the aggregation number of the Py-PEO micelles, which was found to equal 20 ± 2. The combination of the aggregation number found by fluorescence and the hydrodynamic radius found by DLS led to the conclusion that the Py-PEO micelles are made of a hydrophobic pyrene-rich core surrounded by a corona of collapsed PEO chains.

Introduction

A poly(ethylene oxide) chain terminated at one end by a small hydrophobic molecule (hyd-PEO), usually an alkyl chain, is the key structural component of two out of the three families of water-soluble associative thickeners (WSAT) which have achieved commercial acceptance. These two families are the hydrophobically modified ethoxylated urethanes (HEUR) and alkali swellable emulsion copolymers (HASE) with the third one being the hydrophobically modified hydroxyethylcellulose.[1] HEURs are stretches of PEO chains joined together via urethane linkers and terminated at both ends by a hyd-PEO unit. If the urethane linkers are omitted, HEUR molecules can be described as a PEO chain end capped with two hydrophobes (hyd-PEO-hyd).[2] HASEs are comb copolymers where the backbone is a copolymer made of ethyl acrylate and methacrylic acid and the side chains are hyd-PEO molecules.[3]

For both the HEUR[4] and the HASE[5] families, the hydrophilic-to-lipophilic balance (HLB) of the hyd-PEO molecule has been shown to be of paramount importance to controlling the viscoelastic properties of their solutions. Consequently, a considerable body of work has been devoted to the study of model compounds where a monodisperse PEO chain is terminated at either one (α-; hyd-PEO)[6−9] or both (α,ω-; hyd-PEO-hyd)[6−15] ends with a hydrophobic molecule. The general conclusion of these studies is that both the hyd-PEO and hyd-PEO-hyd molecules self-assemble in solution to form micellar structures with a core made of the hydrophobic moieties and a corona consisting of the PEO chains. In the case of hyd-PEO-hyd, the micelles are often referred to as rosettes or flowers. These studies were carried out with a variety of techniques, each technique providing specific information on the system. For instance, ^{1}H NMR provides the self-diffusion coefficient of the molecules,[10,16−18] light scattering yields the hydrodynamic radii of the aggregates,[6,8,12] fluorescence can determine the critical aggregation concentration (CAC) and the aggregation number of the hydrophobic core,[8,9,12,14,19−22] rheology yields the disengagement rate of a hydrophobic moiety from the hydrophobic core of a micelle,[4] and small-angle X-ray (SAXS)[11,13] or neutron (SANS)[7,11,13,14] scattering provides the size of the hydrophobic core and the structural arrangement of the micelles in solution.

Since the peculiar viscoelastic properties of WSATs have led to numerous industrial applications, the behavior of their solutions has been thoroughly studied by rheology. One key result that emerged from all these investigations was to recognize the importance of the hydrophobe, whose absence resulted invariably in a complete loss of the rheological properties of the WSAT solution. The importance attributed to the action of the hydrophobe for rationalizing the viscoelastic behavior of WSAT has led our group[23−26] and others[27−38] to undertake numerous studies where the hydrophobe of a WSAT was replaced by a hydrophobic fluorescent chromophore. This operation allows one to monitor the behavior of the hydrophobe in solution. The chromophore of choice is often pyrene due to the versatility of applications allowed by its fluorescence properties. First of all, the level of hydrophobic associations be-

* To whom correspondence should be addressed.

10.1021/ma047959h CCC: $30.25
Published on Web 03/05/2005

tween pyrenes can be determined experimentally. Upon absorption of a photon, an excited pyrene can either emit fluorescence as a monomer in the blue or, if near to a ground-state pyrene, can form an excimer which emits in the green. Time-resolved fluorescence experiments can distinguish between an excimer formed by diffusional encounters between two single pyrenes and an excimer formed by the direct excitation of a pyrene aggregate. Consequently, the level of aggregation between pyrene pendants can be determined quantitatively by the careful analysis of the pyrene monomer and excimer fluorescence decays.[23−26,31,37,39] A second important aspect of the fluorescence of pyrene resides in its ability to probe the polarity of its local environment so that information can be gained from the fluorescence spectrum of the pyrene monomer on whether the pyrene monomer is probing a hydrophobic or an aqueous environment.[40]

The attraction generated by the numerous photophysical properties of pyrene is unfortunately dampened by the worry that switching from the flexible C_{12-18} alkyl chains typically used for a WSAT to a rigid aromatic chromophore like pyrene could drastically affect the solution properties of the pyrene-labeled WSAT. This is particularly so for studies carried out on HEUR and HASE polymers where the hydrophobes were replaced by pyrene to yield pyrene-labeled HEUR[36−38] and HASE[24] polymers. To the best of our knowledge, the work by Richey et al.[38] represents the only attempt in the literature at characterizing both the rheological behavior and the size of the hydrophobic aggregates of a pyrene-labeled HEUR. In view of the dearth of studies aiming at characterizing pyrene aggregates made from pyrene-labeled WSAT, the association in water of a monodisperse PEO chain labeled at one end with pyrene (Py-PEO) was investigated. Py-PEO in water was found to form micelles whose size and structure were characterized by using a combination of steady-state and time-resolved fluorescence, surface tension, and dynamic light scattering (DLS) experiments. Beside providing some support to the claim that WSATs, where the alkyl chain hydrophobes are replaced with pyrene, behave somewhat like the more typical WSATs, studies such as the present one offer also new means of using fluorescence to characterize the new materials represented by the family of WSATs having rigid hydrophobes.

Throughout this paper, we will compare our results with those of numerous other sources. To do so, a centralized nomenclature was needed. The symbols M*Y*KC*X*, D*Y*KC*X*, M*Y*KPy, and D*Y*KPy were chosen to represent a PEO chain of molecular weight *Y* thousands end-capped at one end with an alkyl chain containing *X* carbon atoms (C*X*), at both ends with a C*X* alkyl chain, at one end with a pyrenyl group, and at both ends with a pyrenyl group, respectively. Following this nomenclature, the Py-PEO sample investigated in this study and made of a 2300 g/mol PEO chain, and a single pyrene hydrophobe would be represented by the symbol M2.3KPy. This nomenclature is similar to that presented in ref 8 and allows one to compare the results obtained with samples characterized in different laboratories.

Experimental Section

Chemicals. Py-PEO shown in Figure 1 was prepared by anionic polymerization at the Dow Chemical Corp., UCAR

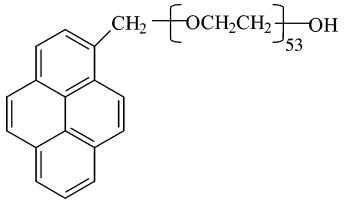

Figure 1. Structure of Py-PEO.

Emulsion Systems. The 1-pyrenemethoxide anion was used to initiate the polymerization, thus ensuring that each Py-PEO molecule bore a single pyrenyl end group. The molecular weight of Py-PEO was determined to be 2600 g/mol from the pyrene content of Py-PEO, which was measured by UV−vis absorption spectroscopy in tetrahydrofuran (THF) using 1-pyrenemethanol as a model compound. This result was confirmed by ^{1}H NMR. The polydispersity index of Py-PEO was estimated to equal 1.1 with a Waters gel permeation chromatograph (GPC) equipped with a Jordi DVB mixed-bed column and an Agilent fluorescence detector. The GPC experiments were performed in THF using polystyrene standards. Hexanes (HPLC grade, Fischer), THF (glass-distilled, Caledon), and acetone (HPLC grade, EM Science) were used as received. Dodecylpyridinium chloride (98%, Aldrich) was recrystallized three times from acetone. Milli-Q water was used to prepare all aqueous solutions.

Polymer Purification and Sample Preparation. Py-PEO was purified by precipitation with hexanes. It was found to be very soluble in water. The stock solutions of Py-PEO were prepared by dissolving a preweighed quantity of purified solid in deionized water.

UV−vis Absorption Measurements. Absorption spectra were acquired on a Hewlett-Packard 8452A diode array spectrophotometer using a cell with a 1 cm path length.

Pyrene Content of Polymer Samples. The pyrene content (λ, in moles of pyrene per gram of polymer) was determined by measuring the absorbance of a solution prepared by dilution of an initial stock solution of known concentration. Associations between ground-state pyrenes are known to distort the absorbance spectrum of pyrene.[41] In the case of THF, which is a good solvent for pyrene, little pyrene−pyrene interactions are expected to occur between the pyrene groups, and the absorption spectra should not be distorted. The pyrene concentration of a polymer solution was then estimated from the absorbance value at 344 nm and the extinction coefficient of 1-pyrenemethanol (ϵ[344 nm, in THF] = 42 700 M^{-1} cm^{-1}). Plotting the absorbance against polymer concentration for several polymer concentrations yields a straight line. The slope gives the pyrene content of the polymer, λ, in moles of pyrene per gram of polymer.

Steady-State Fluorescence Measurements. Fluorescence emission spectra were acquired on a Photon Technology International LS-100 steady-state system with a pulsed xenon flash lamp as the light source. The samples were not deoxygenated due to foam formation. The fluorescence spectra were acquired for polymer concentrations ranging from 0.006 to 150 g/L. At low Py-PEO concentration, a fluorescence microcell (Hellma, with an inner cross section of 3 × 3 mm^2) was used with the usual right angle configuration. For higher Py-PEO concentrations, a triangular cell (Hellma) was used with the front face geometry to prevent the inner filter effect. Emission spectra were acquired by exciting the samples at 344 nm. The fluorescence intensities of the monomer (I_M) and the excimer (I_E) were calculated by taking the integrals under the fluorescence peaks from 372 to 378 nm for the pyrene monomer and from 500 to 530 nm for the pyrene excimer. Choosing these ranges of wavelengths ensures that no residual excimer emission is present at the wavelengths where the monomer fluorescence is being monitored and that no residual monomer emission is present at the wavelengths where the excimer fluorescence is being monitored.

Determination of N_{agg} by Steady-State Fluorescence. Fluorescence is a powerful tool to determine the number of

surfactant molecules per micelle (N_{agg}). In a typical fluorescence experiment, a hydrophobic chromophore (D) and quencher (Q) are added to the surfactant solution. The chromophore and the quencher, being hydrophobic, associate with the hydrophobic core of the surfactant micelle and do not reside in the water phase. Because of the Poisson statistics which rule the distribution of hydrophobic molecules inside micelles, the quantity $\ln(I_0/I)$, where I_0 and I are the fluorescence intensities without and with quencher, equals $\langle n \rangle$, the average number of quenchers per micelle. Since $\langle n \rangle$ equals $[Q_m]/[Mic]$ with [Mic] and $[Q_m]$ being the micelle concentration and the concentration of quencher bound to the micelles, respectively, a plot of $\ln(I_0/I)$ vs the overall quencher concentration, [Q], should yield a straight line for a fixed concentration of surfactant, [S]. This is because the ratio $[Q_m]/[Mic]$ can be rewritten as $K[Q]/(1 + K[Mic])$, where K is the equilibrium constant between quenchers free in solution or bound to the micelles. If the equilibrium constant, K, between free and associated quenchers is known, the slope of this straight line yields N_{agg} because [Mic] is related to N_{agg}, the average number of surfactant molecules per micelle, by the relationship [Mic] = ([S] − cmc)/N_{agg}. These relationships are shown in eq 1. This procedure holds when the rate constant for the quenching of the chromophore is significantly larger than the inverse of the lifetime of the chromophore (i.e., quenching occurs much more quickly than the excited chromophore has time to relax down to the ground state). This procedure originally proposed by Turro and Yekta for quenchers binding tightly to micelles, i.e., for very large K values,[42] has become a standard for the determination of the N_{agg} values of surfactant micelles. In the case of polymeric surfactants bearing more than one hydrophobe, the parameter N_{agg} will represent in this paper the number of hydrophobes forming the core of the micelles.

$$\ln(I_0/I) = \langle n \rangle = \frac{[Q_m]}{[Mic]} = \frac{K[Q]}{1 + K[Mic]} \quad (1)$$

Time-Resolved Fluorescence Spectroscopy. The fluorescence decay profiles were obtained by the time-correlated single photon counting (TCSPC) technique using either a Photochemical Research Associates Inc. System 2000 or an IBH time-resolved fluorometer. For all TCSPC experiments, the excitation wavelength was set at 344 nm. The decay curves were obtained by setting the emission wavelength at 374 nm for the monomer and 510 nm for the excimer. To block potential light scattering leaking through the detection system, filters were used with a cutoff at 370 and 495 nm during acquisition of the fluorescence decays for the monomer and excimer, respectively. The samples were not deoxygenated due to foam formation. At polymer concentrations lower than 1 g/L, fluorescence decays were collected with a right angle configuration. At higher polymer concentrations, the higher optical densities required a front face arrangement to obtain a sufficiently strong fluorescence signal. All fluorescence decays were collected over at least 512 channels. To properly analyze the fluorescence decays, a good signal/noise ratio must be obtained. To this effect, fluorescence decays were acquired with a minimum of 20 000 and 10 000 counts at the maximum of the monomer and excimer fluorescence decays, respectively. Reference decay curves of deoxygenated solutions of PPO [2,5-diphenyloxazole] in cyclohexane ($\tau = 1.42$ ns) and BBOT [2,5-bis(5-*tert*-butyl-2-benzoxazolyl)thiophenel] in ethanol ($\tau = 1.47$ ns) were used for the analysis of the monomer and excimer decay curves, respectively, to account for the wavelength shift of the photomultiplier tube. All fluorescence decays were analyzed with a sum of exponentials.

Dynamic Light Scattering. A Brookhaven BI-200 SM light scattering goniometer equipped with a Lexel 2 W argon ion laser operating at 514.5 nm was used. The refractive index and viscosity of water were taken to be 1.33 and 0.89 mPa·s, respectively. The sample cells were cleaned before each measurement by flushing them in an acetone fountain for 20 min. All measurements were performed at 25 °C at a measurement angle of 90°.

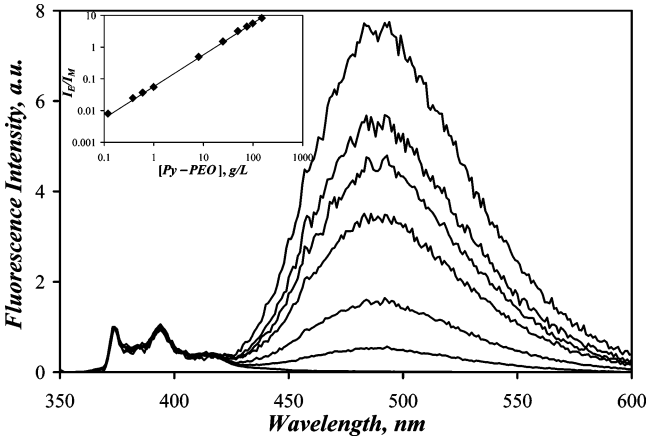

Figure 2. Fluorescence spectra of Py-PEO in water normalized at 375 nm and acquired with Py-PEO concentrations of 0.11, 8, 25, 49, 75, 99, and 150 g/L from bottom to top. The inset shows the corresponding I_E/I_M ratio as a function of Py-PEO concentration. $\lambda_{ex} = 344$ nm.

Surface Tension Measurements. A DuNuoy ring tensiometer was used for the surface tension measurements. The ring was lightly flamed to remove any organic particles clinging to it. Afterward, the ring was cleaned by washing with a soap and water solution and then rinsing with Milli-Q water and methanol and then dried using compressed nitrogen gas. The glass sample vessel was similarly cleaned using soap, water, and methanol and dried using nitrogen gas. The samples were placed into the glass vessel, and the ring was immersed into the solution. The surface tension was measured several times until the same value could be obtained three times in a row. The value was then recorded as the measured surface tension and was corrected by multiplying by a correction factor obtained from a chart supplied by the manufacturer (Central Scientific Co., Inc.). The sample was removed from the vessel, and both the ring and the vessel were cleaned as described above before the next measurement.

Results

The fluorescence spectra of Py-PEO in water were acquired at different Py-PEO concentrations, and they are shown in Figure 2. As more Py-PEO was added to the solution, more excimer was formed, as expected.[43] A log−log plot of the ratio of the fluorescence intensities of the excimer over that of the monomer, I_E/I_M, as a function of Py-PEO concentration is linear with a slope of 0.99, as shown in the inset of Figure 2. Thus, the I_E/I_M ratio is proportional to the Py-PEO concentration. This result, on the other hand, is rather unexpected because a linear increase in the I_E/I_M ratio as a function of pyrene concentration is usually obtained when the excimer formation occurs via diffusional encounters between pyrene moieties.[43] A similar result has been reported for a M5KPy sample where the I_E/I_M ratio has been found to increase linearly with polymer concentration.[44] This result led to the conclusion that excimer of M5KPy formed by diffusion. Yet one should expect some hydrophobic associations to take place between the hydrophobic pyrene units of Py-PEO, i.e., that the excimer is not entirely formed by diffusional encounters. Such questions can be addressed by carrying out time-resolved fluorescence experiments.

To investigate whether the pyrene excimer of Py-PEO is formed by diffusion or ground-state associations, the fluorescence decays of the pyrene monomer and excimer were acquired at different Py-PEO concentrations in water. The fluorescence decays were fitted with a sum of two or three exponentials numbered with the index

Table 1. Parameters Retrieved from the Triexponential Fit of the Pyrene Monomer and Excimer Fluorescence Decays of Varying Py-PEO Concentrations in Water; λ_{ex} = 344 nm, λ_{em} = 374 nm (Monomer), and λ_{em} = 510 nm (Excimer)

Monomer Fluorescence

[PyPEO], g/L	τ_{M1}, ns	a_{M1}	τ_{M2}, ns	a_{M2}	τ_{M3}, ns	a_{M3}	$\langle\tau_M\rangle$, ns	χ^2
0.5	0	0	22.7	0.11	142.0	0.89	129.3	1.07
1	0	0	26.1	0.10	134.3	0.90	123.6	1.10
5	2.7	0.15	25.4	0.11	99.9	0.75	77.6	0.96
10	1.3	0.24	19.6	0.12	86.8	0.64	58.1	0.95
15	3.3	0.15	19.4	0.12	76.8	0.73	59.0	1.12
44	7.6	0.23	37.6	0.12	61.3	0.65	45.9	1.28
100	1.6	0.25	13.1	0.20	48.7	0.55	29.8	1.12
149	N/A	N/A	N/A	N/A	N/A	N/A	N/A	N/A

Excimer Fluorescence

[PyPEO], g/L	τ_{E1}, ns	a_{E1}	τ_{E2}, ns	a_{E2}	τ_{E3}, ns	a_{E3}	$\langle\tau_E\rangle$, ns	χ^2
0.5	2.6	0.29	41.2	0.45	137.9	0.26	55.6	1.16
1	2.8	0.10	39.3	0.56	124.1	0.34	64.4	1.18
5	2.7	0.15	39.4	0.55	89.1	0.30	49.1	1.37
10	3.8	0.18	34.7	0.36	67.9	0.46	44.4	1.25
15	2.7	0.22	29.1	0.24	61.1	0.53	40.3	1.04
44	2.3	0.18	10.1	0.16	53.7	0.66	37.5	1.16
100	2.7	0.21	9.4	0.14	53.1	0.65	36.3	1.27
149	2.6	0.19	11.5	0.17	54.1	0.64	37.3	1.30

i. The preexponential factors a_{Mi} and a_{Ei} and decay times τ_{Mi} and τ_{Ei} retrieved from the fits of the decays of the monomer and excimer, respectively, are listed in Table 1. The average lifetime was calculated as $\sum_i a_{Xi}\tau_{Xi}$, where X stands for either M or E.

As the Py-PEO concentration was increased, noticeable changes in the monomer and excimer decays were found. In the case of the monomer decays, the average lifetime, $\langle\tau_M\rangle$, decreased as more Py-PEO was added. Increasing the Py-PEO concentration from 0.5 to 100 g/L led to a drop in $\langle\tau_M\rangle$ from 140 to 30 ns, which was caused, in large part, by the drop in the long monomer decaytime, τ_{M3}, whose exponential contributed most to the fluorescence decays ($a_{M3} > 0.55$ for all polymer concentrations). Such a decrease in decay time with pyrene concentration is usually an indication that diffusional encounters take place between pyrene moieties to form the excimer.[43] A short decay time, τ_{M1}, is listed in Table 1 for the monomer fluorescence decays of Py-PEO at concentrations larger than 5 g/L. This short decay time can be due to a molecular rearrangement experienced by the pyrene moieties inside a pyrene aggregate or residual light scattering.

The fit of the excimer decays required the use of three exponentials. The excimer decays were acquired for Py-PEO concentrations ranging from 0.5 to 149 g/L. Below 0.5 g/L, the fluorescence signal of the excimer was too small to allow the acquisition of fluorescence decays within a reasonable time (<4 h). The most striking effect displayed by the Py-PEO excimer decays is the absence of a rise time at all polymer concentrations studied as shown in Figure 3. These experiments were carried out on an IBH time-resolved fluorometer which offers a faster time response than the PRA instrument also used in this study. Yet no rise time could be detected in the excimer decays even with this more sensitive instrument. Indeed, none of the excimer preexponential factors listed in Table 1 were negative, contrary to what would be expected if a rise time was present in the excimer decays. Out of all the time-resolved fluorescence experiments carried out on pyrene-labeled PEOs in water reported in the literature,[23,27,37] it is the first example where the excimer formed by a pyrene-labeled PEO does not even exhibit some residual rise time. The absence of a rise time in the Py-PEO excimer decays indicates that a large fraction of the excimer is not produced by diffusion, but from the direct excitation of ground-state pyrene aggregates. These results confirm the presence of pyrene aggregates, i.e., Py-PEO micelles, at Py-PEO concentrations as low as 0.5 g/L, the lowest concentration at which excimer decays were acquired.

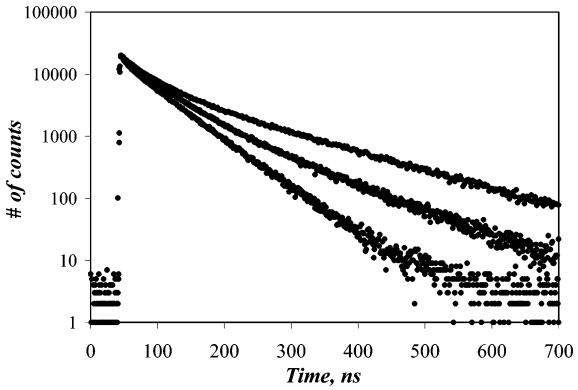

Figure 3. Fluorescence decays of the Py-PEO excimer in water at 0.5 g/L (top), 5 g/L (middle), and 149 g/L (bottom). λ_{ex} = 344 nm, λ_{em} = 510 nm.

At a Py-PEO concentration of 0.1 g/L, residual excimer emission could be observed in the steady-state fluorescence spectrum, but the excimer decay could not be acquired because the signal was too small. In this case, the presence of ground-state pyrene aggregates could be established by acquiring the excitation spectra of the pyrene monomer and excimer. The 0−0 transition was found to occur at 346 and 348 nm in the monomer and excimer excitation spectra, respectively. The 2 nm shift observed when comparing the two excitation spectra is an indication that ground-state pyrene dimers are present,[41] even at this low Py-PEO concentration.

Although the existence of ground-state pyrene aggregates has been demonstrated, the excimer decays also confirm that diffusional encounters take place between the pyrene moieties. This is shown by the parallel decrease of the long decay times τ_{M3} and τ_{E3} with increasing Py-PEO concentration (cf. Table 1). As more Py-PEO is present in solution, the rate of excimer formation by diffusion increases and the decay times associated with excimer formation by diffusion decrease. Furthermore, τ_{M3} and τ_{E3} take similar values as expected when an excimer is formed by the diffusional encounter between two pyrenes. This is because the kinetics of excimer formation by diffusion are coupled for the monomer and excimer and the same decay times are retrieved in both decays.[43] However, above a Py-PEO concentration of 15 g/L, the excimer decays exhibit the same profile regardless of Py-PEO concentration. All decay times and preexponential factors remain constant (cf. Table 1). The main decay time, τ_{E3}, obtained with the strongest preexponential weight takes a value of 54 ± 1 ns, which is very similar to the expected lifetime of the pyrene excimer in water found to equal 55 ± 4, 51 ± 2, 53 ± 3, and 50 ns for pyrene-labeled PEO,[23] HASE,[24] poly(*N*,*N*-dimethylacrylamide),[25] and poly(acrylic acid)[31] in aqueous solutions, respectively.

The absence of a rise time observed in all excimer decays strongly suggests that the excimer is formed

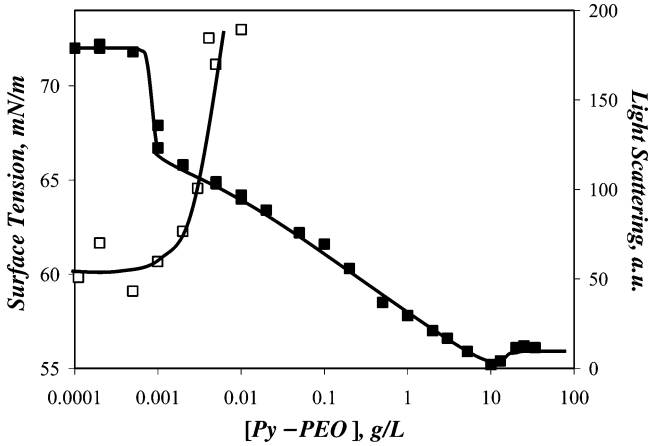

Figure 4. Plot of the surface tension (■) and light scattering intensity (□) of solutions of the Py-PEO surfactant in water.

mostly via the direct excitation of ground-state pyrene aggregates, although some diffusional encounters between pyrene monomers also contribute to excimer formation. At Py-PEO concentrations larger than 15 g/L, the excimer fluorescence decays are unaffected by the Py-PEO concentration. This suggests that excimer formation by diffusional encounters becomes a negligible process in this concentration regime. Consequently, the excimer is being formed by a combination of diffusional encounters and direct excitation of ground-state pyrene aggregates. As the Py-PEO concentration increases, the former mode of excimer formation gives way to the latter. This progressive switch-over seems to be responsible for yielding the linear increase of Py-PEO with increasing Py-PEO concentration shown in the inset of Figure 2. A similar result has been obtained for a related molecule, namely M5KPy.[44] The pyrene aggregates forming the core of the Py-PEO micelles are expected to emit with the lifetime of the pyrene excimer, which is found to equal 54 ± 1 ns in the present study, in agreement with earlier reports.[23−25,31] It is also worth noting that the linear increase of the I_E/I_M ratios with Py-PEO concentration shows no discontinuity over the entire range of Py-PEO concentrations studied (cf. Figure 2). This is an important point which will be used later.

Surface tension is a remarkable tool to determine the critical micellar concentration (CMC) of a surfactant.[45] In the case of polymeric surfactants, the formation of micelles occurs at the critical aggregation concentration, which will be referred to as CAC1 in this paper. The absence of a rise time in the excimer decays acquired down to a Py-PEO concentration of 0.5 g/L demonstrates that Py-PEO micelles are present in this concentration range. Furthermore, the steady-state fluorescence measurements probed the residual presence of pyrene excimer down to pyrene concentrations as low as 0.1 g/L (cf. inset of Figure 2). Such results imply that CAC1 for the formation of Py-PEO micelles must be lower than 0.1 g/L. Consequently, the surface tension of Py-PEO solutions was measured in an effort to determine the CAC1 of Py-PEO. The result of these experiments is shown in Figure 4. Increasing concentrations of Py-PEO induce a sharp drop of the surface tension at a Py-PEO concentration of 0.001 g/L, followed by a continuous decrease of the surface tension which leveled off at a Py-PEO concentration of 10 g/L. The surface tension profile past 0.001 g/L is similar to that of a conventional ionic surfactant such as SDS,[46] for which the concentration where the plateau occurs is taken as the cmc. Thus, the trend shown in Figure 4 would lead to the conclusion that the CAC1 of Py-PEO equals 10 g/L. This is of course not consistent with the fluorescence measurements which confirm the existence of Py-PEO micelles at concentrations much smaller than 10 g/L. Consequently, we attribute the initial drop in surface tension observed at a Py-PEO concentration of 0.001 g/L to the presence of Py-PEO micelles at the surface. Further increasing the Py-PEO concentration leads to the continuous formation of additional Py-PEO micelles at the surface where they contribute to lowering the surface tension. Above 10 g/L, the surface tension probes a second association mechanism, where Py-PEO micelles start to interact and form larger structures. The Py-PEO concentration corresponding to this second transition will be referred as CAC2.

The drop in surface tension seen at a Py-PEO concentration of 0.001 g/L followed by a continuous decrease of surface tension with increasing Py-PEO concentration is not unusual. There are several reports in the literature where the surface tension of poly(styrene-*b*-ethylene oxide)s in water has been shown to exhibit similar features.[47] The trends were due to the formation of polymeric micelles at the surface for bulk concentrations lower than CAC1. Consequently, the drop of surface tension observed in Figure 4 cannot be attributed to CAC1 and CAC1 could be larger than 0.001 g/L. To determine CAC1 in solution, the static light scattering intensity of Py-PEO solutions was measured at 400 nm with the steady-state fluorometer. Figure 4 shows an increase of light scattering intensity above a Py-PEO concentration of 0.003 g/L. This result indicates that Py-PEO molecules aggregate above this concentration in solution and CAC1 of Py-PEO equals 0.003 g/L. The CAC1 value of Py-PEO determined by static light scattering rationalizes why ground-state pyrene dimers are detected by fluorescence at Py-PEO concentrations larger than 0.1 g/L.

To check whether the aggregation of Py-PEO micelles occurs at Py-PEO concentrations larger than 10 g/L as inferred from the surface tension results shown in Figure 4, the size of the Py-PEO species present in solution was investigated by DLS. The DLS autocorrelation functions of Py-PEO in water were acquired, and the size distribution profiles of the Py-PEO aggregates were determined using the CONTIN analysis.[48] They are shown in Figure 5, and a summary of the peak diameters and standard deviations is provided in Table 2. At the lower concentrations of 5.0 and 7.2 g/L, a single peak is observed, indicating the presence of a species 5.6 ± 2.4 nm in diameter. For concentrations of 10 g/L and higher, a bimodal distribution of sizes is obtained with a first peak at 8.0 ± 3.4 nm and a second peak centered at sizes greater than 50 nm. Although there have been reported problems associated with the baseline of the DLS autocorrelation function when using the CONTIN analysis,[49] the results seem consistent with the surface tension results, namely that an aggregation process is taking place in solutions of Py-PEO at concentrations larger than CAC2 = 10 g/L.

Since the fluorescence data demonstrate the presence of pyrene aggregates at Py-PEO concentrations as low as 0.1 g/L, the species with a diameter of 5.6 ± 2.4 nm observed by DLS for Py-PEO concentrations of 5.0 and 7.2 g/L are certainly Py-PEO micelles. They cannot be Py-PEO unimers because a 10 g/L solution of a poly-

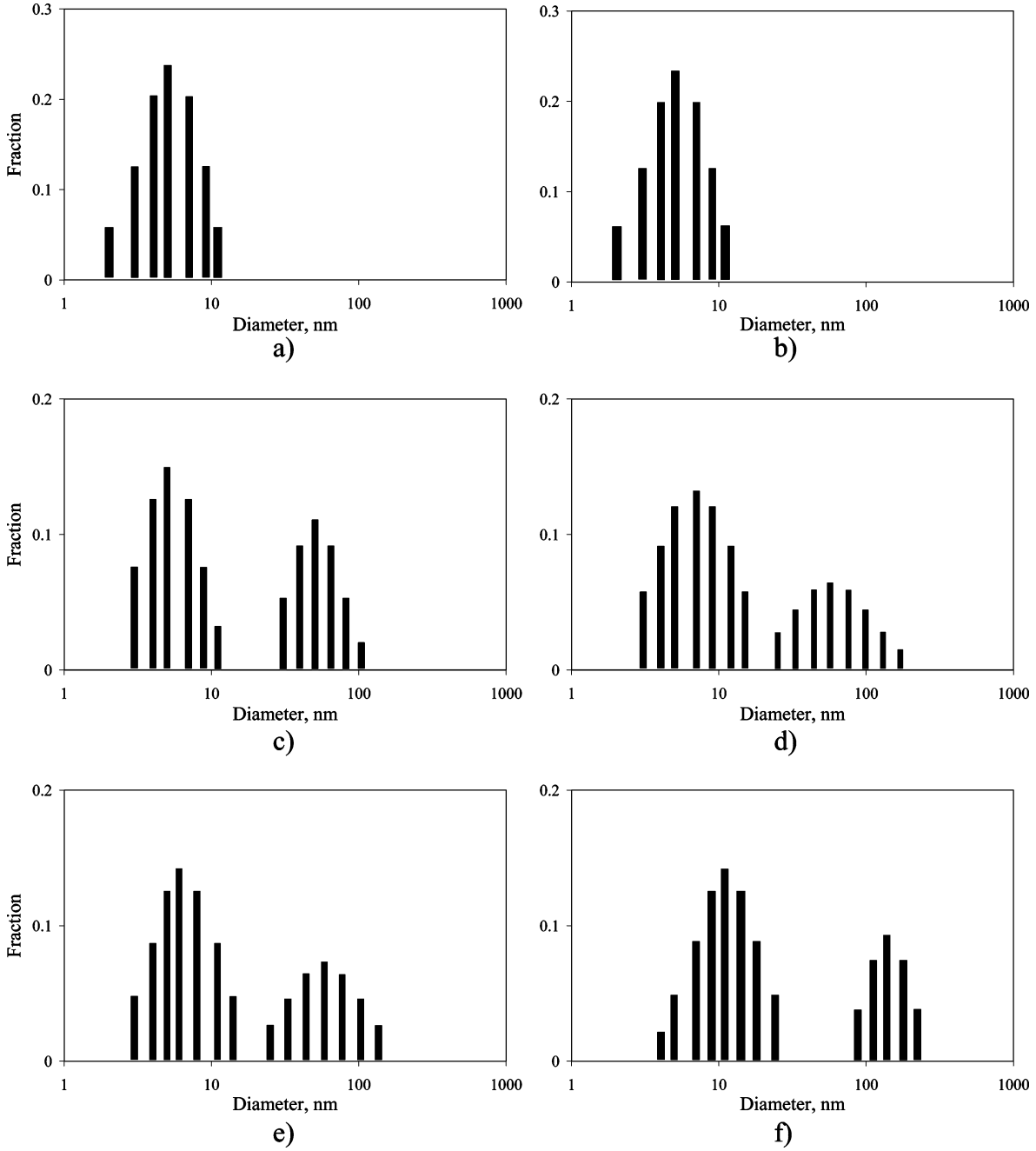

Figure 5. Hydrodynamic diameter distributions obtained by the CONTIN analysis of the DLS autocorrelation functions acquired for Py-PEO in water at concentrations (a) 5.0, (b) 7.2, (c) 10.3, (d) 11.7, (e) 15.4, and (f) 34 g/L.

Table 2. Summary of the Peak Diameters and Their Standard Deviations Obtained from CONTIN Analysis of the DLS Autocorrelation Functions Acquired for Solutions of Py-PEO in Water

[Py-PEO], g/L	⟨peak1⟩, nm	⟨peak2⟩, nm
5.0	5.6 ± 2.4	N/A
7.2	5.6 ± 2.4	N/A
10.3	5.7 ± 2.1	56 ± 19
11.7	7.6 ± 3.5	68 ± 36
15.4	6.9 ± 3.0	65 ± 31
34	11.9 ± 5.1	146 ± 40

(ethylene glycol) with a number-average molecular weight of 2000 g/mol, i.e., similar to the 2300 g/mol molecular weight of the PEO chain of Py-PEO, exhibits no light scattering under the experimental conditions used to acquire the autocorrelation functions for the Py-PEO solutions. Combined with the surface tension trend shown in Figure 4, the DLS results obtained at Py-PEO concentrations larger than 10 g/L suggest that the Py-PEO micelles aggregate into large structures in this concentration range.

The data reported in Figure 5 provide the fraction of scattering intensity arising from particles having a given hydrodynamic radius. Since light scattering intensity increases strongly with particle size, a few large particles can yield a large light scattering intensity. This is indeed the case with the data shown in Figure 5. Although the presence of large structures is observed by DLS, the number fraction of these structures is actually negligible. It must be also noted that the first peak in the histograms shown in Figure 5 shifts with Py-PEO concentration from 5.6 ± 2.4 nm at 5.0 g/L to 11.9 ± 5.1 nm at 34 g/L. However, the spread of the distributions in Figure 5 shows that the species having a smaller hydrodynamic radius overlap substantially

from one histogram to the next. In the Discussion section, the first peak is assumed to correspond to the Py-PEO micelles having a hydrodynamic diameter of 7.2 ± 3.1 nm, when averaged over all DLS experiments. The second peak which is attributed to aggregates of micelles occurs at much larger hydrodynamic diameters, reaching 150 ± 40 nm for a Py-PEO concentration of 34 g/L. This behavior looks like that observed with PEO terminated by aliphatic chains at one end and was explained by a one-step closed association of "flower"-like micelles.[8]

The broad peak obtained by DLS indicates that the Py-PEO micelles exhibit a distribution of sizes. This broadness might question the use of the term "micelles" to describe these polymeric aggregates. However, there are other reports in the literature where hyd-PEO-hyd species were found to exhibit similar size distributions, and their polymeric aggregates were described as micelles.[10,12] Consequently, this terminology is adopted in the present paper.

The aggregation of hyd-PEO and hyd-PEO-hyd micelles such as the one taking place at Py-PEO concentrations larger than CAC2 has been often reported in the literature but, apparently, was found not to perturb much the structure of the micelles.[7,12−14] The aggregates are found to be made of hyd-PEO and hyd-PEO-hyd micelles with their PEO coronas weakly interacting. In one example, the number of hydrophobic units forming a micelle, N_{agg}, was determined by fluorescence as a function of concentration for a monodisperse D20KC12.[12] For this system, N_{agg} was found to fluctuate around 28 ± 3 for polymer concentrations ranging from 14 to 70 g/L despite the fact that micelle aggregates were detected by DLS in this concentration range. Furthermore, the N_{agg} value of 28 ± 3 obtained by fluorescence for D20KC12 compares well with the N_{agg} values of 24 or 38 obtained for monodisperse D6KC12[14] and D12KC12[8] samples, respectively. On the basis of these results and others, it can be concluded that aggregation of hyd-PEO and hyd-PEO-hyd micelles does occur but that the structure of the micelles is not expected to be significantly altered inside an aggregate.[7,12−14]

Steady-state fluorescence was used to determine N_{agg} of the Py-PEO micelles with the Turro−Yekta (TY) method.[42] To do so, a few modifications needed to be made since the hydrophobic core of the Py-PEO micelles is already fluorescent. The absence of a rise time in the pyrene excimer decays (cf. Figure 3) indicates that the pyrene excimer is excited instantaneously upon irradiation. Consequently, instead of adding an external chromophore to probe the Py-PEO micelles, the intrinsic fluorescence of the pyrene excimer was used for that purpose. Dodecylpyridinium chloride (DPC) was chosen as a quencher of the pyrene excimer. The proposed procedure was quite appealing because emission from an excimer signals the presence of a pyrene aggregate. To the best of our knowledge, it is the first time that such a procedure has been implemented.

Significant quenching of the pyrene excimer was observed at DPC concentrations lower than the cmc of DPC in water (1.5×10^{-2} M) for Py-PEO concentrations ranging from 15 to 150 g/L. Although aggregation of the Py-PEO micelles takes place in this concentration range (cf. surface tension and light scattering measurements), the linear increase of the I_E/I_M ratio as a function of Py-PEO concentration (cf. inset of Figure 2) demonstrates

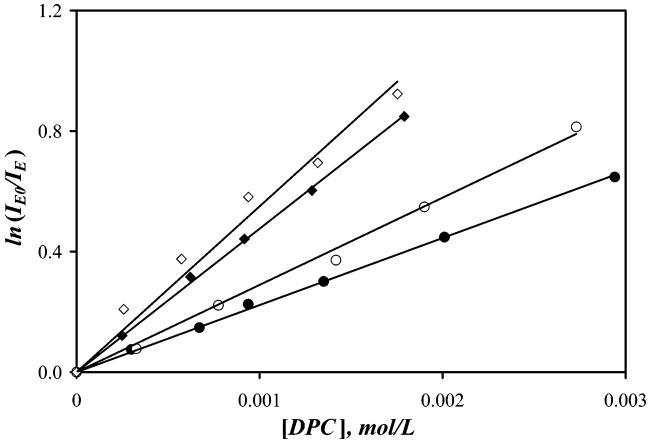

Figure 6. Plots of $\ln(I_{E0}/I_E)$ as a function of DPC concentration for Py-PEO concentrations of 15 (◇), 44 (◆), 100 (○), and 150 g/L (●).

that the core of the Py-PEO micelles is unaffected for these Py-PEO concentrations. If a rearrangement of the pyrene core of the Py-PEO micelles were to take place upon micelle aggregation, the I_E/I_M ratio would be affected. This was not observed. Furthermore, the N_{agg} value of some hyd-PEO-hyd micelles has been determined by fluorescence while the micelles were aggregated, and the reported values were very reasonable.[12] Last but not least, the determination of N_{agg} for surfactant micelles assumes that the concentration of unassociated surfactant molecules remains constant above the cmc and equal to the cmc. Although the CAC1 of Py-PEO was found to equal 0.003 g/L, a substantial monomer emission, indicative of unassociated Py-PEO molecules, can be seen in all fluorescence spectra shown in Figure 2. Although such a large fluorescence contribution of monomer emission might be a consequence of the fluorescence quantum yield of the pyrene aggregates being much smaller than that of a pyrene monomer,[35] it would seem more appropriate to perform the fluorescence quenching experiments in a Py-PEO concentration range where the fraction of free Py-PEO monomer is insignificant. The presence of free Py-PEO molecules has been shown to be negligible for concentrations larger than 15 g/L since the excimer fluorescence decays remain unchanged for Py-PEO concentrations above 15 g/L (cf. Table 1). Consequently, fluorescence spectra of Py-PEO solutions were acquired with increasing amounts of DPC for four Py-PEO concentrations, namely 15, 44, 100, and 150 g/L. DPC was found to target mostly the Py-PEO micelles since little quenching of the pyrene monomer was observed whereas the excimer fluorescence decreased substantially. Following the TY method, the quantity $\ln(I_{E0}/I_E)$ was plotted as a function of DPC concentration, yielding a series of straight lines. These trends are shown in Figure 6.

To determine the nature of the mode of quenching of the pyrene aggregates by DPC, the fluorescence decays of the Py-PEO excimer were acquired on the PRA time-resolved fluorometer as a function of DPC concentration for a Py-PEO concentration of 44 g/L. The decays were fitted with a sum of two exponentials, and the preexponential factors and decay times retrieved from the fits are listed in Table 3. The absence of the short decay time of 2.8 ± 0.4 ns observed in the excimer fluorescence decays of the Py-PEO solutions without quencher acquired with the IBH system (cf. Table 1) are a result of the poorer temporal resolution of the PRA time-

Table 3. Parameters Retrieved from the Biexponential Fit of the Pyrene Excimer Fluorescence Decays of Aqueous Solutions of Py-PEO Surfactant Quenched with DPC ([Py-PEO] = 44 g/L, λ_{ex} = 344 nm, λ_{em} = 510 nm)

[DPC], mmol/L	a_{E1}	τ_{E1}, ns	a_{E2}	τ_{E2}, ns	χ^2
0.00	0.19	7.1	0.81	58	1.08
0.05	0.21	7.4	0.79	58	1.06
0.13	0.21	9.1	0.79	57	1.15
0.20	0.22	9.1	0.78	57	0.89
0.31	0.22	9.3	0.78	56	1.06
0.56	0.29	9.4	0.71	56	1.20
0.71	0.32	8.2	0.68	55	1.18
0.99	0.38	8.7	0.62	55	1.15

resolved fluorometer. In any case, the results listed in Table 3 demonstrate that the long decay time, τ_{E2}, remains unchanged at 56 ± 2 ns upon addition of the DPC quencher. This value is similar to the decay time of 54 ± 1 ns obtained with the IBH fluorometer and corresponds to the lifetime of the pyrene excimer in water.

That the long lifetime of the chromophore remains constant as a function of quencher concentration while the steady-state fluorescence intensity drops substantially is a hallmark of static quenching taking place and strongly supports the use of the TY procedure to determine the N_{agg} value of the Py-PEO micelles. On the other hand, the preexponential factor of the short decay time, τ_{E1}, equal to 9 ± 1 ns increases in weight with DPC concentration. Since τ_{E1} is substantially smaller than τ_{E2}, quenching of the excimer occurs on a rapid time scale. Thus, the method proposed by TY should apply to the Py-PEO system.

According to eq 1, the slopes of the straight lines shown in Figure 6 equal $K/(1 + K[\text{Mic}])$. Taking the inverse of the slope yields eq 2.

$$\text{slope}^{-1} = \frac{1}{K} + \frac{[\text{Py-PEO}] - \text{CAC1}}{N_{agg}} \qquad (2)$$

The CAC1 of Py-PEO was determined to equal 0.003 g/L and can be neglected for the range of concentrations where the quenching fluorescence experiments were performed. According to eq 2, a plot of slope^{-1} as a function of the Py-PEO concentration is expected to yield a straight line whose slope and intercept equal N_{agg}^{-1} and K^{-1}, respectively. Such a plot is shown in Figure 7, and a straight line is indeed obtained. According to the intercept and slope values of the straight line, N_{agg} and K are found to equal 20 ± 2 and 665 ± 60 M^{-1}, respectively.

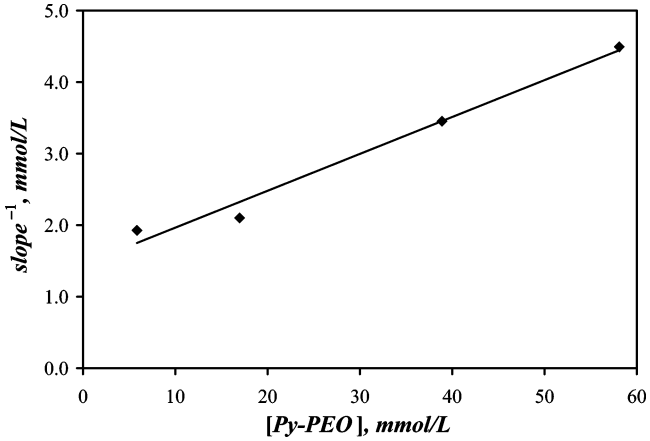

Figure 7. Plot of slope^{-1} obtained from the straight lines shown in Figure 6 vs Py-PEO concentration.

Discussion

The picture that emerges from the measurements reported in the Results section is that the Py-PEO micelles form at concentrations as low as 0.5 g/L since no rise time is observed in the excimer decays (cf. Table 1 and Figure 3). The increase in static light scattering intensity observed at low Py-PEO concentration in Figure 4 suggests that the CAC1 equals 0.003 g/L. The continuous decrease of surface tension observed in Figure 4 is believed to be due to the presence of entire Py-PEO micelles at the surface of the solution.[47] In solution, the Py-PEO micelles are at equilibrium with some Py-PEO unimers whose presence is probed by our fluorescence measurements (cf. Figure 2). As the concentration of Py-PEO increases, more Py-PEO micelles form and the I_E/I_M ratio increases (cf. inset of Figure 2). The Py-PEO micelles are probed by DLS at Py-PEO concentrations lower than 10 g/L (cf. Figure 5). Above 10 g/L, the surface tension plateaus which is a clear indication that aggregation is taking place at larger Py-PEO concentrations. This is confirmed by DLS which shows the presence of large aggregates at Py-PEO concentrations larger than 10 g/L, a concentration which is assigned to CAC2. In the case of Py-PEO, these large aggregates are believed to be made of intact Py-PEO micelles because their formation does not affect the I_E/I_M trend shown in Figure 2. The hydrodynamic diameter of the Py-PEO micelles obtained by DLS is estimated to equal 7.2 ± 3.1 nm when averaged over the diameters corresponding to all smaller species probed by the DLS experiments shown in Figure 5. Because the Py-PEO micelles appear to not be affected upon aggregation, fluorescence quenching experiments were performed at Py-PEO concentrations ranging from 15 to 150 g/L to determine N_{agg} for Py-PEO micelles using the procedure proposed by TY and applying it for the first time to the fluorescence of a pyrene aggregate. A N_{agg} value of 20 ± 2 Py-PEO units per micelle was found. DPC bound weakly to the pyrene core of the Py-PEO micelles with a binding constant equal to 665 ± 60 M^{-1}.

To this date, there is no other instance where N_{agg} of pyrene aggregates made by pyrene-labeled WSATs in water has been determined. The only other study where a pyrene-labeled WSAT was used to determine an N_{agg} value was for a HEUR polymer where the hydrophobes had been replaced with pyrene.[38] The N_{agg} value was obtained by monitoring the excimer fluorescence intensity of mixtures of the pyrene-labeled HEUR with a typical commercial HEUR thickener and assuming that both thickeners have the same aggregation properties. We believe that the present study is superior because it yields the N_{agg} value of pyrene aggregates by applying the well-established TY procedure and without making any additional assumption.

The N_{agg} value of WSATs is a highly sought after parameter because it provides a measure of the size of the hydrophobic domains of a WSAT. Consequently, numerous techniques have been applied toward the determination of the N_{agg} value of HEUR systems. Earlier reports using fluorescence on a polydisperse D30KPy[38] and ^{1}H NMR on polydisperse D28KC814, D6KC16, and D6KC18[17] led to N_{agg} values ranging from 2 to 6. However, later studies have found larger N_{agg} values (>10) for similar systems.[7,8,14,21,22] Furthermore, there have been several examples where the N_{agg} value was found to be the same for M*Y*KC*X* and D2×*Y*KC*X*.

In other words, the architecture of the micelles depends essentially on the hydrophilic-to-lipophilic balance (HLB). For instance, monodisperse M16KC16[7] and D32KC16[8] with the same HLB have been reported to have both a N_{agg} value equal to 34. Their hydrodynamic radii were similar and equaled 15.5 and 17.5 nm for M16KC16 and D32KC16, respectively.[9] Interestingly, a N_{agg} value of 28 was found by another research group for a monodisperse D35KC16.[22] The closeness of these results reflects agreement in the more recent literature that model HEUR systems form hydrophobic domains consisting of several tens of units, as found for the Py-PEO molecule.

Yet experiments and theory indicate that N_{agg} increases when the HLB decreases.[50] Although many such studies have been performed with PEO chains of different length terminated with a C12 alkyl chain instead of a C16 alkyl chain more similar to the pyrenyl hydrophobe, one would expect a M2.3KC16 molecule to form micelles with an N_{agg} value much larger than 28, 34, or 34 as found for D35KC16,[22] D32KC16,[8] and M16KC16,[7] respectively. This is because the HLB is much higher for M2.3KC16 than for D35KC16, D32KC16, and M16KC16. Thus, the N_{agg} value of 20 ± 2 obtained for Py-PEO appears to be rather low. This result might be a consequence of the geometry of the pyrene molecule whose rigidity might disfavor an efficient packing of the hydrophobes. Poor packing of the pyrenes might yield a pyrene aggregate made of 20 units having a core volume larger than that of a hydrophobic aggregate made of a larger number of more efficiently packed C16 alkyl chains.

Our earlier statement that the structure of the Py-PEO micelles is not affected upon aggregation is supported by earlier studies carried out on PEO surfactant micelles using scattering techniques.[7,12−14] These studies demonstrated that the micelles made by a series of monodisperse HEUR with hexadecyl[7] or dodecyl[12] hydrophobes form clusters, where the PEO coronas of the micelles weakly interact with each other. More importantly, the structure of the micelles, i.e., a hydrophobic core surrounded by a PEO corona, was preserved inside the aggregates. However, the core radius has been reported to increase slightly with polymer concentration as $[Poly]^{0.09}$ when the surfactant concentration is larger than the overlap concentration C^*.[7] Below C^*, the radius of the core, and thus N_{agg}, are expected to remain constant.[7,51] Consequently, C^* of Py-PEO was estimated using eq 3, as done in ref 7.

$$C^* = \frac{N_{agg} M_P}{\frac{4}{3}\pi N_A {R_H}^3} \quad (3)$$

In eq 3, N_A is the Avogadro number, R_H is the hydrodynamic radius, and M_P represents the polymer molecular weight if dealing with hyd-PEO aggregates, or half the polymer molecular weight, when dealing with hyd-PEO-hyd aggregates. Using the D_H value of 7.2 nm found by DLS, the N_{agg} value of 20 found by fluorescence quenching, and the molecular weight, M_P, of the unimer equal to 2600 g/mol for Py-PEO, C^* was found to equal 440 g/L. This value is extremely large when compared to that of other systems (for instance, 50 g/L for M16KC16),[7] and this is certainly due to the short PEO chain of the Py-PEO sample which makes the micelles more compact. Nevertheless, since all fluorescence quenching experiments were conducted at Py-PEO concentrations smaller than C^*, the core of the Py-PEO micelles is expected to remain constant, and the N_{agg} value of 20 ± 2 found by our fluorescence quenching experiments should be valid.

According to the DLS measurements, the Py-PEO micelles exhibit a hydrodynamic diameter D_H of 7.2 ± 3.1 nm. The fluorescence quenching experiments yielded a N_{agg} value of 20 ± 2. Since the DLS and fluorescence quenching techniques report two different structural information on the Py-PEO micelles, it is important to investigate what implications a D_H value of 7.2 nm and a N_{agg} value of 20 have for the structure of the Py-PEO micelles. To do so, the Py-PEO micelles are pictured as having a core/shell structure where the hydrophobic core is made of pyrene moieties, whereas the shell consists of the PEO chains. The core and the shell are assumed to exhibit a spherical geometry. The methods used to determine the core radius and the shell thickness are discussed separately.

Two approaches are adopted to estimate the core radius, and they are based on two extreme views of the packing of the pyrene core. The first extreme assumes that the pyrene moieties are tightly packed and that the pyrene-made core is crystalline. According to the reported pyrene crystal structure, a crystal unit cell has a volume of 1.035 nm^3 and contains four pyrene molecules.[52] Consequently, one pyrene moiety occupies a volume of 0.259 nm^3, and 20 such units will fill up a spherical core with a radius of 1.1 nm. The other extreme assumes that the pyrene moieties are loosely packed and uses their encounter radius, found by fluorescence to equal 0.8 nm,[53] as a measure of their size inside the core. In this case, 20 spherelike pyrene units with an encounter radius of 0.8 nm will make up a spherical core with a radius of 2.2 nm. Consequently, the pyrene core is expected to exhibit a diameter ranging from 2.2 to 4.4 nm, depending on the packing efficiency of the pyrene moieties inside the pyrene aggregate.

The size of the shell of the Py-PEO micelles can be estimated by considering the possible conformations of the PEO chains. To do so, the sizes of the building blocks making up the PEO chain of the Py-PEO molecules must be determined. The PEO chain of Py-PEO consists of 53 ethylene oxide units. The Kuhn length (l_K) of PEO has been estimated to equal 0.707 nm, and the number of segments N_K of a PEO chain of molecular weight M_P was estimated to equal $0.0141 M_P$.[54] Consequently, a PEO chain consisting of 53 ethylene oxide units is made of $N_K = 33$ segments of Kuhn length 0.707 nm.

Theory derived for star polymers[55] or block copolymer micelles[56] predicts that when many chain ends are forced to encounter at a tight focal point, they stretch into the solution and adopt an extended conformation. If the PEO chains were to adopt a fully stretch conformation, they would exhibit a full length of $N_K \times l_K = 33 \times 0.707 = 23$ nm. The diameter of the corona would then range between 49 and 51 nm, depending on the compactness of the core. This value is much too large to account for the D_H values of 7.2 nm recovered by DLS for the Py-PEO micelles. Consequently, the PEO chains of the Py-PEO micelles do not adopt a fully extended conformation.

Since theory predicts that the PEO chains adopt an extended conformation with respect to the unperturbed size of the PEO chain,[55,56] the size of the unperturbed chain must be estimated in order to have a reference point. To do so, one can determine the radius of gyration

R_G of an unperturbed PEO chain made of 33 segments. R_G equals $(1/6)^{0.5} \times 33^{0.5} \times 0.707 = 1.65$ nm. Assuming that the PEO chains remain unperturbed, the corona would have a thickness of $2 \times 1.65 = 3.3$ nm, and the diameter of the Py-PEO micelles would range from 8.8 up to 11.0 nm. Similar conclusions are reached when using the hydrodynamic radius, R_H, of the PEO chain which can be determined to equal 1.3 or 1.4 nm whether one uses the relationship $R_H = 0.145M_w^{0.571}$ or the intrinsic viscosity, respectively.[57,58] Using either value of R_H would yield diameters for the Py-PEO micelles ranging from 7.4 up to 10.0 nm Whether these values are obtained with R_G or R_H, they represent a lower estimate of the micellar diameter since the chains are assumed to be unperturbed. In the corona, the PEO segments are expected to expand which would lead to larger diameter values. Nevertheless, the diameters retrieved from the analysis are slightly larger than the 7.2 nm value found for the hydrodynamic diameter of the Py-PEO micelles. This result leads to the conclusion that the PEO chains in the Py-PEO corona adopt a conformation which is similar to or slightly more compact than that of the unperturbed polymer coil. In other words, the framework of the theory developed for star-shaped polymers or block copolymer micelles does not apply to the Py-PEO micelles investigated in the present study. Indeed, when the concentration profile proposed by Daoud and Cotton for star polymers[55] is implemented for the PEO chains in the corona to determine the shell thickness,[59] the diameter of the Py-PEO micelles was found to equal 17 nm, much too large to agree with our DLS results.

Since our experimental results suggest that the PEO chains are not extended around the pyrene core, the thickness of the PEO shell was estimated by considering that each segment of the PEO chain was a spherical bead of volume $(4/3)\pi(l_K/2)^3$ and calculating the volume occupied by $N_K \times N_{agg} = 33 \times 20 = 660$ such beads tightly packed in the corona. Noting that the volume of the corona is equal to that of the Py-PEO micelle (R) minus that of the core (R_C), the radius of the micelle is found according to eq 4:

$$R = \left(R_C^{\,3} + 660\left(\frac{0.707}{2}\right)^3\right)^{1/3} \qquad (4)$$

If the radius of the core is 1.1 nm, the diameter of the Py-PEO micelle is found to equal 6.2 nm and the surface of the core is covered by 2.8 layers 0.707 nm thick of tightly packed beads. If the radius of the core is 2.2 nm, the diameter of the Py-PEO micelle equals 6.8 nm and the surface of the core is covered by 1.7 layers.

The diameters obtained by assuming a tight packing of the PEO segments wrapping around the pyrene core agree well with the hydrodynamic diameter of 7.2 ± 3.1 nm determined by DLS. It supports our suggestion that the PEO chains are not extended at the surface of the hydrophobic core. It is assumed that the reason for this compactness resides in the necessity of shielding the hydrophobic pyrene core from the water. Indeed, the 20 PEO chains making up the corona of the Py-PEO micelles barely allow 2−3 layers of PEO beads to cover the pyrene core which seems to be a minimum coverage to prevent contact between the pyrene core and water. Consequently, our results suggest that the PEO chains of the Py-PEO micelles choose to lose entropy to pack tightly around the pyrene core in order to gain free energy by minimizing the unfavorable contacts between the hydrophobic pyrene core and the water. This study represents a first attempt at describing the pyrene aggregates generated by a PEO chain labeled at one end with pyrene.

The above discussion is based on the values of N_{agg} and the hydrodynamic diameter averaged over the total number of particles present in solution. Clearly, a more accurate picture of the Py-PEO micelles would have been obtained if the distribution of sizes observed by DLS had been considered. Unfortunately, such a consideration is hampered by the absence of information about the width of the distribution of N_{agg} values because this information cannot be obtained by fluorescence quenching experiments.

Conclusions

Experiments carried out with surface tension, DLS, steady-state fluorescence quenching, and time-resolved fluorescence decays led to the conclusion that Py-PEO micelles consist of 20 Py-PEO molecules. The hydrophobic pyrenes self-assemble into the core of the micelles, which is covered by 2−3 layers of tightly packed PEO beads. Surface tension and static light scattering measurements indicate that Py-PEO micelles form at very low polymer concentrations around 0.003 g/L. Their existence in the bulk is inferred from static light scattering measurements (cf. Figure 4), the steady-state fluorescence spectra which exhibit some excimer fluorescence at Py-PEO concentration as low as 0.1 g/L, the linear increase of the I_E/I_M ratio as a function of Py-PEO concentration, and the excimer fluorescence decays which were acquired for polymer concentrations above 0.5 g/L and which exhibit no rise time at any polymer concentration (cf. Figure 3). The hydrodynamic diameter of the Py-PEO micelles was determined by DLS and was found to be around 7 nm. At polymer concentrations larger than 10 g/L, surface tension and DLS experiments demonstrated that the Py-PEO micelles aggregate into larger entities. Since this aggregation is not probed by steady-state fluorescence, it does not affect the pyrene cores and the aggregation number of the Py-PEO micelles is expected to remain unchanged. Fluorescence quenching measurements performed at polymer concentrations larger than 15 g/L yielded an aggregation number of 20 units/micelle. This is a reasonable value when compared to the N_{agg} values of 34, 34, 18, and 28 obtained for M16KC16,[7] D32KC16,[7−9] D33KC16,[22] and D35KC16,[22] respectively, where the C16 hydrophobe has the same number of carbon atoms as pyrene. This N_{agg} value combined with the hydrodynamic diameter determined by DLS led to the conclusion that the PEO chains are not extended, as the model for star polymers[55] or block copolymer micelles[56] predicts, but form a compact shell around the hydrophobic core to shield it from water. Beside providing a detailed description of a hyd-PEO system where the alkyl chain typically used as the hydrophobe was replaced with a rigid and planar molecule, this study represents also the first example where the intrinsic fluorescence of the pyrene excimer is used to determine the N_{agg} value of micelles where the hydrophobic moiety of the surfactant is pyrene.

References and Notes

(1) Lundberg, D. J.; Glass, J. E.; Eley, R. R. *J. Rheol.* **1991**, *35*, 1255−1274.
(2) Winnik, M. A.; Yekta, A. *Curr. Opin. Colloid Interface Sci.* **1997**, *2*, 424−436.

(3) Jenkins, R. D.; DeLong, L. M.; Bassett, D. R. *Hydrophobic Polymers. Performance with Environmental Acceptability*; Glass, J. E., Ed.; Advances in Chemistry No. 248; American Chemical Society: Washington, DC, 1996; pp 425−447.
(4) Annable, T.; Buscall, R.; Ettelaie, R.; Whittlestone, D. *J. Rheol.* **1993**, *37*, 695−726.
(5) Tirtaatmadja, V.; Tam, K. C.; Jenkins, R. D. *Macromolecules* **1997**, *30*, 3271−3282. Tam, K. C.; Guo, L.; Jenkins, R. D.; Bassett, D. R. *Polymer* **1999**, *40*, 6369−6379.
(6) Chassenieux, C.; Nicolai, T.; Durand, D. *Macromolecules* **1997**, *30*, 4952−4958.
(7) Beaudoin, E.; Borisov, O.; Lapp, A.; Billon, L.; Hiorns, R. C.; François, J. *Macromolecules* **2002**, *35*, 7436−7447.
(8) Gourier, C.; Beaudoin, E.; Duval, M.; Sarazin, D.; Maître, S.; François, J. *J. Colloid Interface Sci.* **2000**, *230*, 41−52.
(9) Beaudoin, E.; Hiorns, R. C.; Borisov, O.; François, J. *Langmuir* **2003**, *19*, 2058−2066.
(10) Chassenieux, C.; Nicolai, T.; Durand, D.; François, J. *Macromolecules* **1998**, *31*, 4035−4037.
(11) François, J.; Maître, S.; Rawiso, M.; Sarazin, D.; Beinert, G.; Isel, F. *Colloids Surf. A* **1996**, *112*, 251−265.
(12) Alami, E.; Almgren, M.; Brown, W.; François, J. *Macromolecules* **1996**, *29*, 2229−2243.
(13) Abrahmsén-Alami, S.; Alami, E.; François, J. *J. Colloid Interface Sci.* **1996**, *179*, 20−33.
(14) Alami, E.; Rawiso, M.; Isel, F.; Beinert, G.; Binana-Limbele, W.; François, J. In *Hydrophilic Polymers. Performances and Environmental Acceptability*; Glass, J. E., Ed.; Advances in Chemistry No. 248; American Chemical Society: Washington, DC, 1996; pp 343−362.
(15) Kaczmarski, J. P.; Glass, J. E. *Macromolecules* **1993**, *26*, 5149−5156.
(16) Nyström, B.; Walderhaug, H.; Hansen, F. K. *J. Phys. Chem.* **1993**, *97*, 7743−7752.
(17) Walderhaug, H.; Hansen, F. K.; Abrahmsén, S.; Persson, K.; Stilbs, P. *J. Phys. Chem.* **1993**, *97*, 8336−8342.
(18) Uemura, Y.; Macdonald, P. M. *Macromolecules* **1996**, *29*, 63−69.
(19) Yekta, A.; Duhamel, J.; Adiwidjaja, H.; Brochard, P.; Winnik, M. A. *Langmuir* **1992**, *9*, 881−883.
(20) Yekta, A.; Duhamel, J.; Adiwidjaja, H.; Brochard, P.; Winnik, M. A. *Macromolecules* **1993**, *26*, 1829−1836.
(21) Yekta, A.; Xu, B.; Duhamel, J.; Adiwidjaja, H.; Winnik, M. A. *Macromolecules* **1995**, *28*, 956−966.
(22) Yekta, A.; Nivaggioli, T.; Kanagalingam, S.; Xu, B.; Masoumi, Z.; Winnik, M. A. In *Hydrophilic Polymers. Performances and Environmental Acceptability*; Glass, J. E., Ed.; Advances in Chemistry Series No. 248; American Chemical Society: Washington, DC, 1995; pp 363−376.
(23) Lee, S.; Duhamel, J. *Macromolecules* **1998**, *31*, 9193−9200.
(24) Prazeres, T. J. V.; Beingessner, R.; Duhamel, J.; Olesen, K.; Shay, G.; Bassett, D. R. *Macromolecules* **2001**, *34*, 7876−7884.
(25) Kanagalingam, S.; Ngan, C. F.; Duhamel. J. *Macromolecules* **2002**, *35*, 8560−8570.
(26) Kanagalingam, S.; Spartalis, J.; Cao, T.-M.; Duhamel, J. *Macromolecules* **2002**, *35*, 8571−8577.
(27) Char, K.; Frank, C. W.; Gast, A. P. *Macromolecules* **1989**, *22*, 3177−3180. Char, K.; Frank, C. W.; Gast, A.; Tang, W. T. *Macromolecules* **1987**, *20*, 1833−1838.
(28) Quina, F.; Abuin, E.; Lissi, E. *Macromolecules* **1990**, *23*, 5173−5175.
(29) Yoshida, K.; Morishima, Y.; Dubin, P. L.; Mizusaki, M. *Macromolecules* **1997**, *30*, 6208−6214. Morishima, Y.; Mizusaki, M.; Yoshida, K.; Dubin, P. L. *Colloids Surf., A* **1999**, *147*, 149−159. Mizusaki, M.; Morishima, Y. *J. Phys. Chem. B* **1998**, *102*, 1908−1915.
(30) Schillén, K.; Anghel, D. F.; Miguel, M. D. G.; Lindman, B. *Langmuir* **2000**, *16*, 10528−10539.
(31) Seixas de Melo, J.; Costa, T.; Miguel, M. D. G.; Lindman, B.; Schillén, K. *J. Phys. Chem. B* **2003**, *107*, 12605−12621.
(32) Maltesh, C.; Somasundaran, P. *Langmuir* **1992**, *8*, 1926−1930.
(33) Chandar, P.; Somasundaran, P.; Turro, N. J. *Macromolecules* **1988**, *21*, 950−953.
(34) Winnik, F. M.; Ringsdorf, H.; Venzmer, J. *Langmuir* **1991**, *7*, 912−917. Ringsdorf, H.; Venzmer, J.; Winnik, F. M. *Macromolecules* **1991**, *24*, 1678−1686. Winnik, F. M.; Regismond, S. T. A.; Goddard, E. D. *Langmuir* **1997**, *13*, 111−114. Winnik, F. M.; Winnik, M. A.; Tazuke, S. *J. Phys. Chem.* **1987**, *91*, 594−597.
(35) Anghel, D. F.; Alderson, V.; Winnik, F. M.; Mizusaki, M.; Morishima, Y. *Polymer* **1998**, *39*, 3035−3044. Anghel, D. F.; Toca-Herrera, J. L.; Winnik, F. M.; Rettig, W.; v. Klitzing, R. *Langmuir* **2002**, *18*, 5600−5606. Siu, H.; Duhamel, J. *J. Phys. Chem. B* **2005**, *109*, 1770−1780.
(36) Hu, Y.-Z.; Zhao, C.-L.; Winnik, M. A. *Langmuir* **1990**, *6*, 880−883.
(37) Duhamel, J.; Yekta, A.; Hu, Y.-Z.; Winnik, M. A. *Macromolecules* **1992**, *25*, 7024−7030.
(38) Richey, B.; Kirk, A. B.; Eisenhart, E. K.; Fitzwater, S.; Hook, J. *J. Coat. Technol.* **1991**, *63*, 31−40.
(39) Duhamel, J.; Kanagalingam, S.; O'Brien, T.; Ingratta, M. *J. Am. Chem. Soc.* **2003**, *125*, 12810−12822. Zhang, M.; Duhamel, J.; van Duin, M.; Meessen, P. *Macromolecules* **2004**, *37*, 1877−1890. Picarra, S.; Duhamel, J.; Fedorov, A.; Martinho, J. M. G. *J. Phys. Chem. B* **2004**, *108*, 12009−12015.
(40) Winnik, F. M.; Regismond, S. T. A. *Colloids Surf. A: Physicochem. Eng. Aspects* **1996**, *118*, 1−39.
(41) Winnik, F. M. *Chem. Rev.* **1993**, *93*, 587−614.
(42) Turro, N. J.; Yekta, A. *J. Am. Chem. Soc.* **1978**, *100*, 5951−5952.
(43) Birks, J. B. *Photophysics of Aromatic Molecules*; Wiley: New York, 1970; p 351.
(44) Eckert, A. R.; Hsiao, J.-S.; Webber, S. E. *J. Phys. Chem.* **1994**, *98*, 12025−12031.
(45) Attwood, D. *Kolloid Z. Z. Polym.* **1969**, *232*, 788−792. Elworthy, P. H.; Macfarlane, C. B. *J. Pharm. Pharm.* **1962**, *14*, 100−102. Corkill, J. M.; Goodman, J. F.; Ottewill, R. H. *Trans. Faraday Soc.* **1961**, *57*, 1627−1636.
(46) Jönsson, B.; Lindman, B.; Holmberg, K.; Kronberg, B. *Surfactants and Polymers in Aqueous Solution*; Wiley: New York, 1998; p 255.
(47) Nakamura, K.; Endo, R.; Takeda, M. *J. Polym. Sci., Polym. Phys. Ed.* **1976**, *14*, 1287−1295. Dewhurst, P. F.; Lovell, M. R.; Jones, J. L.; Richards, R. W.; Webster, J. R. P *Macromolecules* **1998**, *31*, 7851−7864.
(48) Provencher, S. W. *Comput. Phys. Comm.* **1982**, *27*, 229−242.
(49) Ruf, H.; Gould, B. J.; Haase, W. *Langmuir* **2000**, *16*, 471−480.
(50) François, J.; Beaudoin, E.; Borisov, O. *Langmuir* **2003**, *19*, 10011−10018.
(51) Birshtein, T. M.; Zhulina, E. B. *Polymer* **1989**, *30*, 170−177.
(52) Robertson, J. M.; White, J. G. *J. Chem. Soc* **1947**, 358−68.
(53) Duhamel, J.; Winnik, M. A.; Baros, F.; André, J. C.; Martinho, J. M. G *J. Phys. Chem.* **1992**, *96*, 9805−9810.
(54) Pattanayek, S. K.; Juvekar, V. A. *Macromolecules* **2002**, *35*, 9574−9585.
(55) Daoud, M.; Cotton, J. P. *J. Phys. (Paris)* **1982**, *43*, 531−538.
(56) Halperin, A. *Macromolecules* **1987**, *20*, 2943−2946.
(57) *Polymer Handbook,* 4th ed.; Brandrup, J., Immergut, E. H., Grulke, E. A., Eds.; Wiley: New York, 1999.
(58) Devanand, K.; Selser, J. C. *Macromolecules* **1991**, *24*, 5943−5947.
(59) Pham, Q. T.; Russel, W. B.; Thibeault, J. C.; Lau, W. *Macromolecules* **1999**, *32*, 2996−3005.

MA047959H